CHITOSAN AS A POLYMERIC SCAFFOLD FOR THE AGGREGATION OF MESO-TETRAKIS(4-SULPHONATOPHENYL)PORPHINE

Andriy Synytsya [a], *Alla Synytsya* [b], *Petra Blafková* [a], *Martin Maryška* [c], *Jana Ederová* [d], *Jiří Spěvaček* [e], *Jana Čopíková* [a], *Karel Volka* [b], *Vladimír Král* [b]

[a] Department of Carbohydrate Chemistry and Technology, [b] Department of Analytical Chemistry, [c] Department of Glass and Ceramics, [d] Central Laboratories, Institute of Chemical Technology in Prague, Technická 5, 166 28 Prague 6, Czech Republic

[e] Institute of Macromolecular Chemistry of the Academy of Science, Heyrovského nám. 2, 162 06 Prague 6, Czech Republic

Abstract

Interaction of *meso*-tetrakis(4-sulphonatophenyl)porphine ($TPPS_4$) with chitosan was studied previously in aqueous solutions [1]. It was reported that an addition of the polysaccharide at appropriate concentrations and pH values induce and support pH-dependent self-aggregation of the macrocycles. An addition of powder porphyrin to chitosan solution (pH ~7 and 2) led to the rapid formation of coloured precipitates assigned as chitosan/$TPPS_4$ complexes **1** and **2**. Spectroscopic methods (vis-NIR, FT-IR, Raman and ^{13}C CP-MAS NMR) confirmed that in both these complexes porphyrin macrocycles are highly aggregated. H- and J-aggregates of $TPPS_4$ were indicated respectively in **1** and **2**. Elemental analysis and solid state NMR showed that complex **1** contain more chitosan (8.3–11.1 units per macrocycle) than **2** (5.8–7.5 units per macrocycle). According to the results of thermal analysis (DSC and TG) both complexes are less thermostable than initial chitosan and may undergo two step thermal degradation of a polysaccharide part. Light microscopic images indicated fibrous structure of **1** and lamellar structure of **2**, while electronic microscopy showed that both complexes consist of spherical nanoparticles of similar shape and size (~20–50 nm). Structural difference between the complexes could be explained by dissimilar self-assembling ways of supramolecular structures.

Introduction

Self-assembly provides a primary mechanism through which ordered structures in both natural and artificial systems are created. The adsorption of self-assembled structures on solid surfaces is one of the fundamental processes for the development of molecule-based nanodevices [2]. Polymer template has some advantages in preparation of such supramolecular systems. It gives shape and directionality for the growth of ordered structures. As chiral molecules, biopolymers are able to impose chirality on the self-assembly of molecular aggregates. Self-aggregation in aqueous systems is a common feature of water-soluble porphyrins carrying polar or charged substituents [3-5]. Moreover, such macrocycles are able to form supramolecular highly ordered structures onto the surface of oppositely charged biopolymers – polypeptides [6], proteins [2, 7, 8], nucleic acids [9-11] or the components of mitochondrial membranes [12]. Therefore, electrostatic interaction between these macrocycles and polymeric scaffold could promote self-forming ordered arrays. As a model cationic polysaccharide, chitosan may be interesting for interaction experiments with water-soluble macrocycles carrying anionic groups. It has been reported earlier [1] that chitosan induce and enhance pH-dependent self-aggregation of *meso*-tetrakis(4-sulphonatophenyl)porphine ($TPPS_4$) in aqueous solution. It has been also found that at appropriate conditions a formation of solid

porphyrin-chitosan complexes is possible. Such complexes are interesting as self-assembling ordered structures that could be used, for example, as water disinfection agent like it has been reported for porphyrins immobilised on chitosan membrane [13]. In this work solid aggregates of $TPPS_4$ macrocycles on chitosan macromolecules were prepared and analysed by spectroscopic, microscopic and thermal methods.

Material and Methods

Materials

Sodium salt of *meso*-tetrakis(4-sulphonatophenyl)porphyrin and medium molecular weight chitosan (M_r = 400 kD, *DD* = 21.2 mol. %) originated from crab shell α-chitin were purchased from Fluka, Germany. Concentrated solution of chitosan (4 % m/v in 0.1 M HCl) was prepared on re-distilled water and the pH values were adjusted to 6.8 and 2.3 by drop-wise addition of 0.1 M NaOH and measured by a Marrison model 90 pH/temperature meter. Final concentration of work chitosan solutions was 2 % m/v.

Preparation of solid porphyrin/chitosan complexes

Small amounts (50 mg) of solid $TPPS_4$ were added into flacks containing 10 ml of work chitosan solutions (pH 6.8 and 2.3). Coloured precipitates were isolated, washed twice with the medium and than wash with methanol. Finally, the precipitates were dried on glass surface. Obtained solid products were assigned as $TPPS_4$/chitosan complexes **1** (pH 6.8) and **2** (pH 2.3).

Spectroscopic measurements

Diffusion reflectance Vis-NIR spectra (400–1200 nm) of the samples in MgO tablets were measured by NIRSystem 6500 spectrometer. FT-IR spectra (4000–400 cm^{-1}) of the samples in KBr tablets were recorded on Perkin Elmer FTIR spectrometer 1760X; accumulation 64 scans, spectral resolution of 4 cm^{-1}. Dispersion Raman spectra were recorded on Dilor-Jobin Yvon-Spex Raman spectrometer equipped with Argon Ion Laser System (λ_{ex} = 632 nm, excitation power 16 mW) and Olympus BX 40 system microscope with 10× objective. Raman spectra were measured in 10 aliquot solutions (5 accumulations per one aliquot) at 24 °C, exposure time for one accumulation was 60 s. FT-Raman spectra were recorded on Bruker FT-Raman (FRA 106/S, Equinox 55/S) spectrometer equipped with a Nd:YAG laser (λ_{ex} =1064 nm, excitation power 240 mW), quartz beam splitter and Ge detector (cooled with liquid N_2); accumulation 2300 scans, resolution 4 cm^{-1}. High-resolution ^{13}C CP/MAS NMR spectra were measured on Bruker Avance 500 spectrometer at 125.8 MHz with spinning frequency 11 kHz and contact time 2 ms. ^{13}C scale was calibrated using the external standard glycine (176.03 ppm – low field carbonyl signal).

Microscopic measurements

The microscopic samples of complexes **1** and **2** were put onto the sample glass under the objective 4 of microscope Nicon SM2-2T equipped with Intralux 4000-1 lamp, colour camera and digitizer Micro-Movies. Images were focused, digitised and decomposed into pixels using 256-dot scale. The samples were also deposited on carbon tape, sprayed by carbon and put under the objective of cold field emission scanning electron microscope Hitachi S-4700 (Hitachi, Japan) at working distance 12 mm, integrated electron detector, resolution 2.1 nm at accelerating voltage 1 kV.

Thermal analysis

TG analysis of the complexes and the initial compounds was made with TG-750 Stanton-Redcroft instrument. DSC measurements were done with DSC131 Setaram instrument. Heating rate was 10°C/min in both cases; temperature range was 25–900 °C for TG, 25–695 °C for DSC. The complexes heated to intermediate temperatures (245 °C – both complexes, and 200 °C – only complex **2**) and then cooled to room temperature were analysed by FT-IR.

General methods

Organic elemental analysis of the $TPPS_4$/chitosan complexes was made by Analyser 2400, CHNS/O, series II. The degree of deacetylation (*DD*, mol. %) of used chitosan was determined by first derivative (1D) UV spectroscopic method [14].

Results and Discussion

Organic elemental analysis

Results of organic elemental analysis of the $TPPS_4$/chitosan complexes **1** and **2** are summarised in Table 1. The contents of porphyrin and polysaccharide components as well as chitosan to $TPPS_4$ molar ratios were calculated from sulphur and nitrogen contents. Obtained values confirmed that complex **1** contained less porphyrin and more chitosan than complex **2**.

Table 1: Results of elemental analysis of $TPPS_4$/chitosan complexes **1** and **2**

Samples	C (%)	H (%)	N (%)	S (%)	Porfyrin (%)	Chitosan (%)	Chit./Porf. molar ratio*
1	43.15	5.84	6.48	4.81	35.02	52.61	8.3
2	39.47	5.47	5.74	5.38	39.22	40.93	5.8

* calculated on monomeric units of chitosan.

Vis-NIR spectra

The diffuse reflectance Vis-NIR spectra of solid $TPPS_4$, chitosan and the $TPPS_4$/chitosan complexes are shown in Fig. 1A. The visible region (400–900 nm) of the spectrum of free porphyrin is quite different from that of corresponding spectra of both complexes. For both porphyrin and its complexes with chitosan the spectral region consists of highly overlapped spectral features.

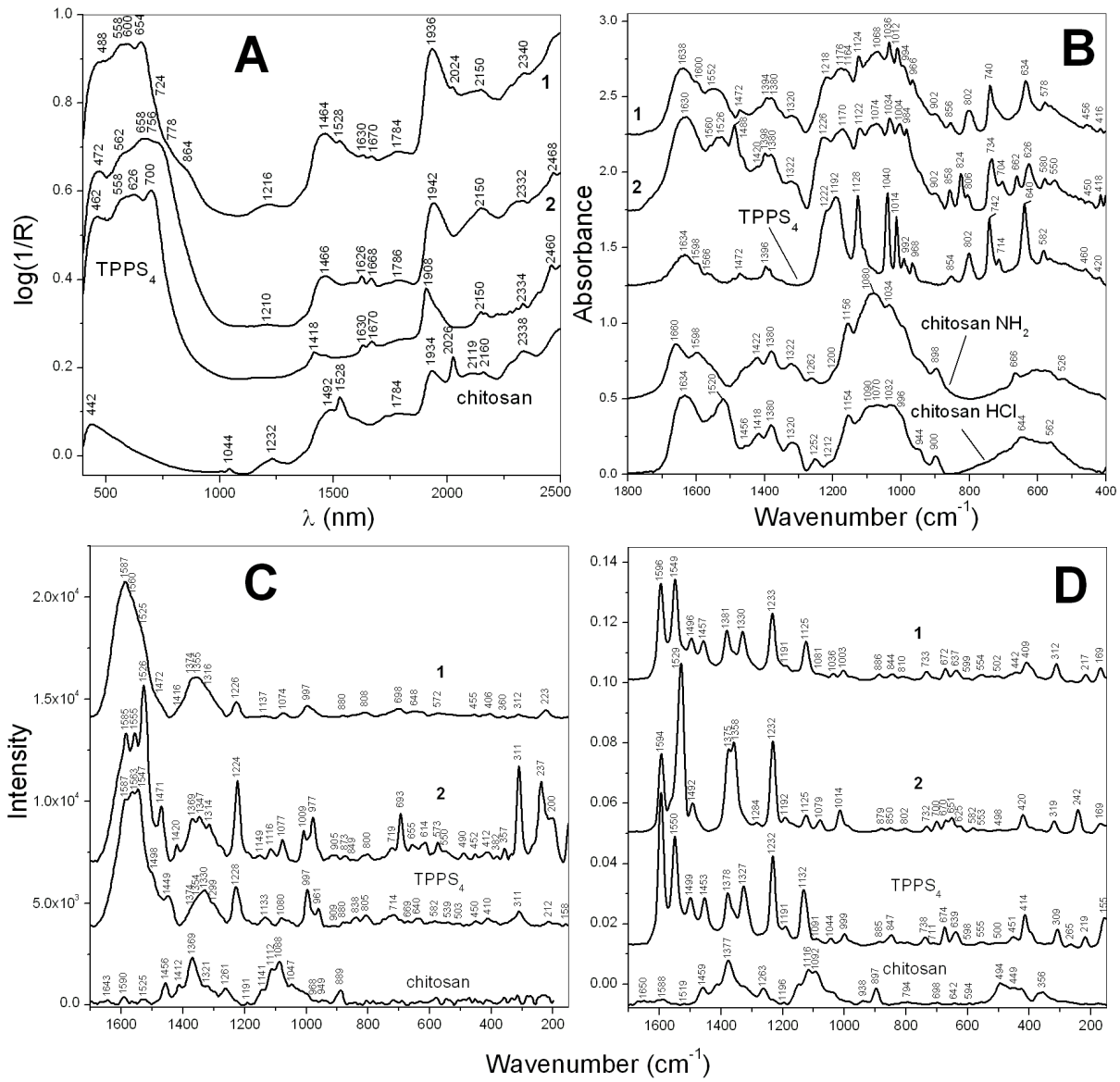

Figure 1 : Vis-NIR (A), FT-IR (B), visible-excited Raman (C) and FT-Raman (D) spectra of $TPPS_4$, chitosan and $TPPS_4$/chitosan complexes **1** and **2**

Complex **1** showed several intense bands centred at 488, 558, 600 and 654 nm and several weaker shoulders in the region of 700–900 nm. The nature of the first band and the shoulders is unclear, while the last three maximums could be assigned to Q-bands of H-aggregated macrocycles. Corresponding bands of chitosan-bound stacked $TPPS_4$ species in aqueous solutions have been found at 558–560, 595 and 650–660 nm [1]. Complex **2** showed highly overlapped bands centred at 472, 562, 685 and 756 nm. The last two spectral features may indicate J-aggregated macrocycles, which showed solution Q-band at 700–706 nm according to earlier reports [1]. The NIR region (900–2500 nm) of the spectra of $TPPS_4$ and chitosan showed several characteristic bands, which were also found in the spectra of complexes. The polysaccharide bands at 1528, 1784, 2026 and 2338 nm were more pronounced for complex **1**, while the porphyrin features at 1630, 1670, 2150, 2334 and 2460 nm for complex **2**. This difference is indicative for the $TPPS_4$/chitosan ratio in these complexes and, similar to the results of elemental analysis, leads to assumption that complex **1** contains more chitosan and less porphyrin than complex **2**.

FT-IR spectra

FT-IR spectra of $TPPS_4$, chitosan and the $TPPS_4$/chitosan conjugates **1** and **2** are shown in Fig. 1B. The spectra of both complexes contain IR bands originated from porphyrin and chitosan parts. For the complex **2**, the IR bands at 1004, 984 and 806 cm^{-1} assigned to the porphyrin modes are significantly red shifted (by 4–10 cm^{-1}) in comparison with corresponding bands of $TPPS_4$. The intense IR bands of **2** at 1488, 1034, 858, 824, 734, 704 and 662 cm^{-1} were assigned to phenyl substituents of the macrocycles [15]. These bands are enhanced and shifted in comparison with corresponding bands of $TPPS_4$. Both porphyrin and phenyl marker bands of complex **1** generally show smaller shifts in their positions. The IR spectrum of $TPPS_4$ showed two strong bands at 1192 cm^{-1} (with a shoulder at 1222 cm^{-1}) and 1128 cm^{-1} assigned respectively to $\nu_{as}(SO_3^-)$ and $\nu_s(SO_3^-)$ vibrations of ionised sulphonato groups. These bands showed significant changes in their position and intensity in the spectra of the complexes. IR bands and shoulders of the complexes at 1656–1660, 1556–1558, 1420, 1380, 1320–1322, 1154–1164, 1068–1074, 942 and 902 cm^{-1} were assigned to chitosan vibrations. The spectrum of complex **1** has a shoulder at 1600 cm^{-1}, which is characteristic for NH_2 groups of chitosan in free base form. In contrast, two broad bands of complex **2** at 1630 and 1526 cm^{-1}, which were assigned respectively to $\nu_{as}(NH_3^+)$ and $\nu_s(NH_3^+)$ vibrations, indicate chitosan in cationic form.

Raman spectra

Dispersion and FT Raman spectra of $TPPS_4$, chitosan and $TPPS_4$/chitosan complexes are shown in Fig. 1 (C, D). Porphyrin skeletal modes predominate in the spectra of both porphyrin and the complexes, while some phenyl modes were also observed; the bands of chitosan were insignificant and overlapped by intense bands of macrocycles. Band assignment was made according to the literature [15, 16]. Position and intensity of the porphyrin bands have evident changes in the $TPPS_4$/chitosan complexes. The C_β-C_β stretching modes ν_2 (1547–1550 cm^{-1}) and ν_{11} (~1500 cm^{-1}) showed significant downshifts (21 and 7–10 cm^{-1}) in complex **2**, and the bands of C_α-C_m stretching modes (1563, 1420–1471 cm^{-1}) also altered their positions. The porphyrin modes ν_{20} (1354, 1327–1330 cm^{-1}) and ν_9 (~1133, 1080–1091 cm^{-1}) involving mainly C_β-H deformations showed significant red shift (4–18 cm^{-1}). Large upshift (9–16 cm^{-1}) was observed for pyrrole breathing modes ν_6 (961–977 cm^{-1}) and ν_{15} (997–999 cm^{-1}) in complex **2**. Two very intense and sharp bands at 311 and 237 cm^{-1}, assigned respectively to ν_8 and γ_{16} modes of the porphyrin core, were found in the visible-excited Raman spectrum of complex **2**. These modes are forbidden in the Raman spectra of free base $TPPS_4$ [15]. Protonation of porphyrin ring leads to lowering $TPPS_4$ symmetry from D_{4h} to D_{2d}, and ν_8 and γ_{16} modes have the same A_1 symmetry and are resonantly enhanced via the Frank-Condon mechanism [15, 16]. According to Tsuboi's rules such resonance enhancement is the strongest for these two modes because the resonance excitation causes the largest displacement along their coordinates [15]. In the spectra of complex **2** the band of phenyl mode π_3 at 693–700 cm^{-1} was found to be enhanced, and the ν_7 mode of $TPPS_4$ found at 880–885 cm^{-1} was shifted to

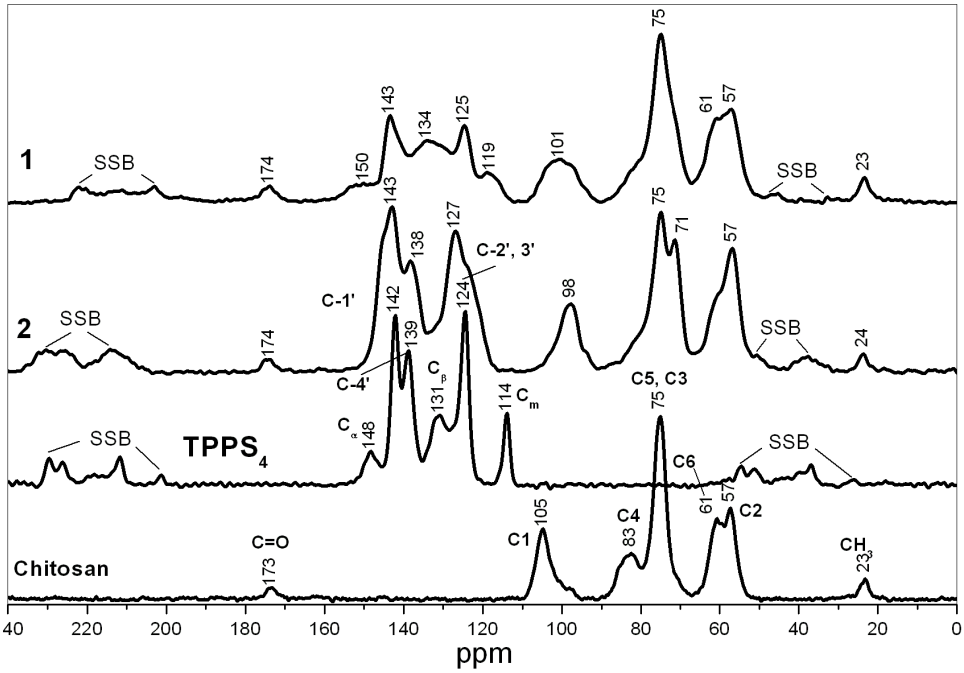

Figure 2 : ^{13}C CP-MAS NMR spectra of $TPPS_4$, chitosan and $TPPS_4$/chitosan complexes

lower frequency by 6–7 cm^{-1}. The latter mode involves C_m-Ph stretch, so its downshift may indicate weakened C_m-Ph bonds in this complex [15, 16]. In addition, the band at ~640 cm^{-1} assigned to phenyl in-plane deformation φ_9 split into bands at 651–655 and 614–625 cm^{-1}. This spectral change could be explained by non-equivalence of phenyls owing to electrostatic interaction of sulphonato groups with chitosan or other macrocycle. Therefore, observed alteration in Raman spectra upon $TPPS_4$/chitosan complexation at different pH values confirm structural changes in macrocycles owing to aggregation onto the polysaccharide scaffold as well as, in the case of **2**, protonation of the pyrrolic nitrogens.

^{13}C CP/MAS NMR spectroscopy

Solid state ^{13}C NMR spectra of $TPPS_4$, chitosan and $TPPS_4$/chitosan complexes are shown in Fig. 2. Assignment of carbon peaks for porphyrin and chitosan standards were made according to literature [17, 18]. The NMR spectra of complexes **1** and **2** showed carbon resonance signals of both chitosan and porphyrin components in separated regions. The chitosan to porphyrin molar ratios of the complexes calculated on the basis of carbon peak areas were 11.1 for **1** and 7.5 for **2**. Therefore, the complex prepared at stronger acidic conditions contains more porphyrin molecules. The NMR values are something smaller than those of organic elemental analysis that maybe due to the contribution of SSB into the whole area of porphyrin bands. The chitosan region (50–110 ppm) of complex **1** is similar to that of the initial chitosan in free base form, but C-1 carbon signal was broadened and shifted upfield by 4.3 ppm. In addition, C-4 carbon resonance decreased and a non-resolved upfield shoulder appeared at 71 ppm. This shoulder assigned to shifted signal of some C-3 carbons, together with broadened C-1 carbon resonance, indicate partial ionisation of chitosan. Complex **2** showed more pronounced changes of chitosan carbon resonances. Both C-1 and C-3 carbon signals are markedly shifted upfield respectively by 7 and 3.8 ppm. The C-6 carbon signal is slightly upfield shifted and overlapped to the signal of C-2 carbon centred at 57 ppm. New shifted bands are attributive to ionised monomeric units of chitosan. Therefore, according to NMR spectra non-amidated units of chitosan macromolecules are partially ionised in neutral complex **1** and almost ionised in acidic complex **2**. The porphyrin region (110–160 ppm) is less resolved for both the complexes in comparison to the $TPPS_4$. In complex **1** all the resonance signals of porphyrin core carbons are markedly broadened and downfield shifted by ~2–5 ppm, whereas the signals of phenyl carbons demonstrated weaker broadening and slight shifts. In complex **2** the resonances of pyrrolic carbons are upfield shifted, while meso-carbons are shifted downfield. Such shifts led to

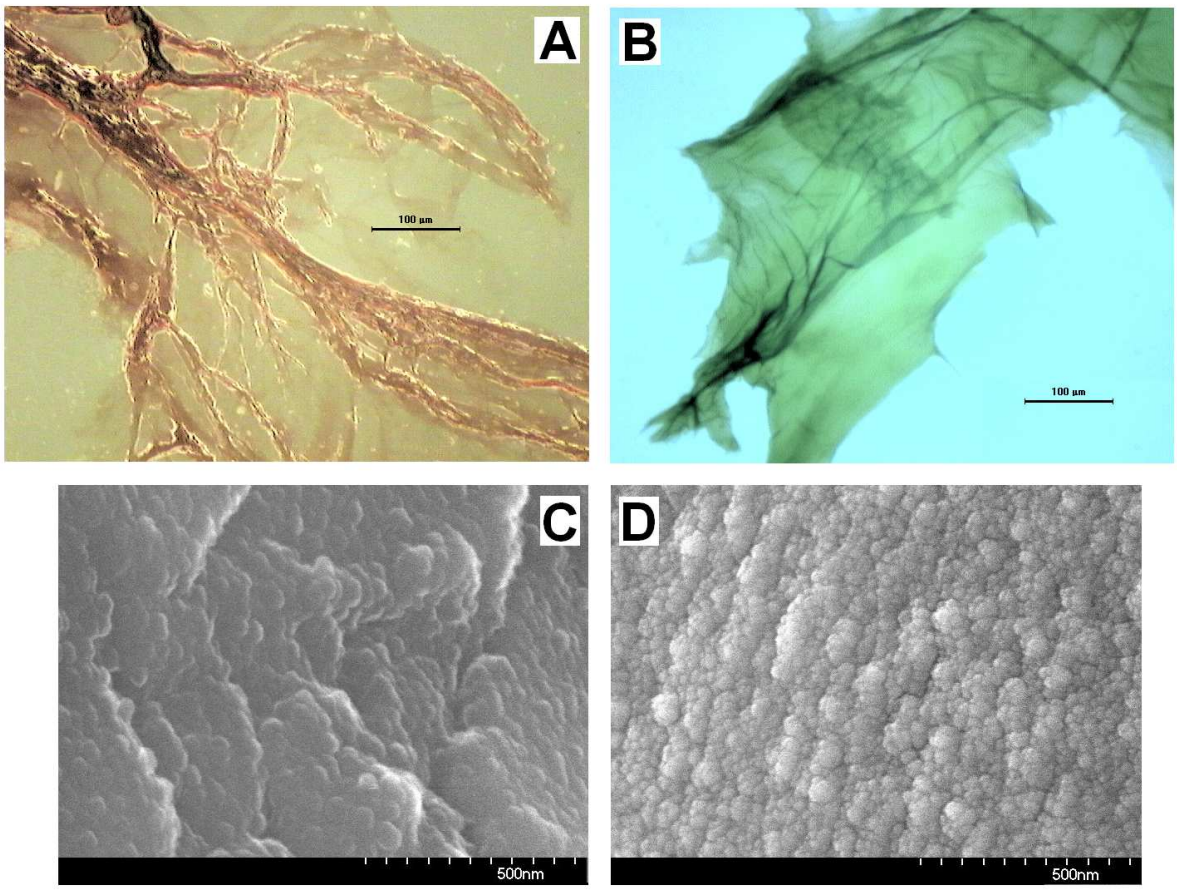

Figure 3 : Light (top) and electronic (bottom) microscopic images of $TPPS_4$/chitosan complexes **1** (A, C) and **2** (B, D)

overlapping of the porphyrin core carbon resonances with more intense signals of phenyl carbons. Several peaks or shoulders were assigned to C_β and/or C_m porphyrin carbons that could be explained by existence of non-equivalent pyrrols in the complexes as a result of macrocycle deformation via stacking (complex **1**) or protonation and electrostatic interaction with sulphonato groups of neighbour porphyrin molecules (complex **2**). Significant shifts of phenyl carbon signals were also observed for both complexes: C-1', 4' downfield by 1.3–1.9 ppm for complex **1** and C-2', 3' downfield by 2.5 ppm for complex **2**. These changes could be explained by decrease in the angle between the macrocycle and the phenyl rings as a result of aggregation and/or protonation.

Light and electronic microscopy

Fig. 3 shows light and electronic microscopic images of solid $TPPS_4$/chitosan complexes **1** and **2**. The complex **1** obtained in weak acidic conditions performs wreathed thread-like structures (Fig. 3A). According to the image scale, the average diameter of a single thread is ~5 µm. Fig. 3B represents the image of complex **2** obtained at pH 2.5. This complex forms layer structures, and the thickness of a layer is ~3 µm. Electronic images of both these complexes (Fig. 3C, D) show spherical nanoparticles of diameter ~20–50 nm, which are assembled into more complex structures, fibres or lamellas dependently on pH. Evident difference between solid microstructures of these two complexes could be a result of diverse ways of porphyrin binding onto chitosan macromolecules at neutral and acidic conditions.

Thermal analysis

Thermogravimetric (TG, DTG) and differential scanning calorimetric (DSC) curves of complexes **1** and **2** are shown in Fig. 4A-C. The first large change in the slope of the TG curves and corresponding first endothermic peak in the DSC curves are associated with the evaporation of water present in the samples. Comparing with chitosan (DTG: 328 °C; DSC: exothermic peak at 310 °C), the weight-loss of complexes was shifted to lower temperatures concomitantly with

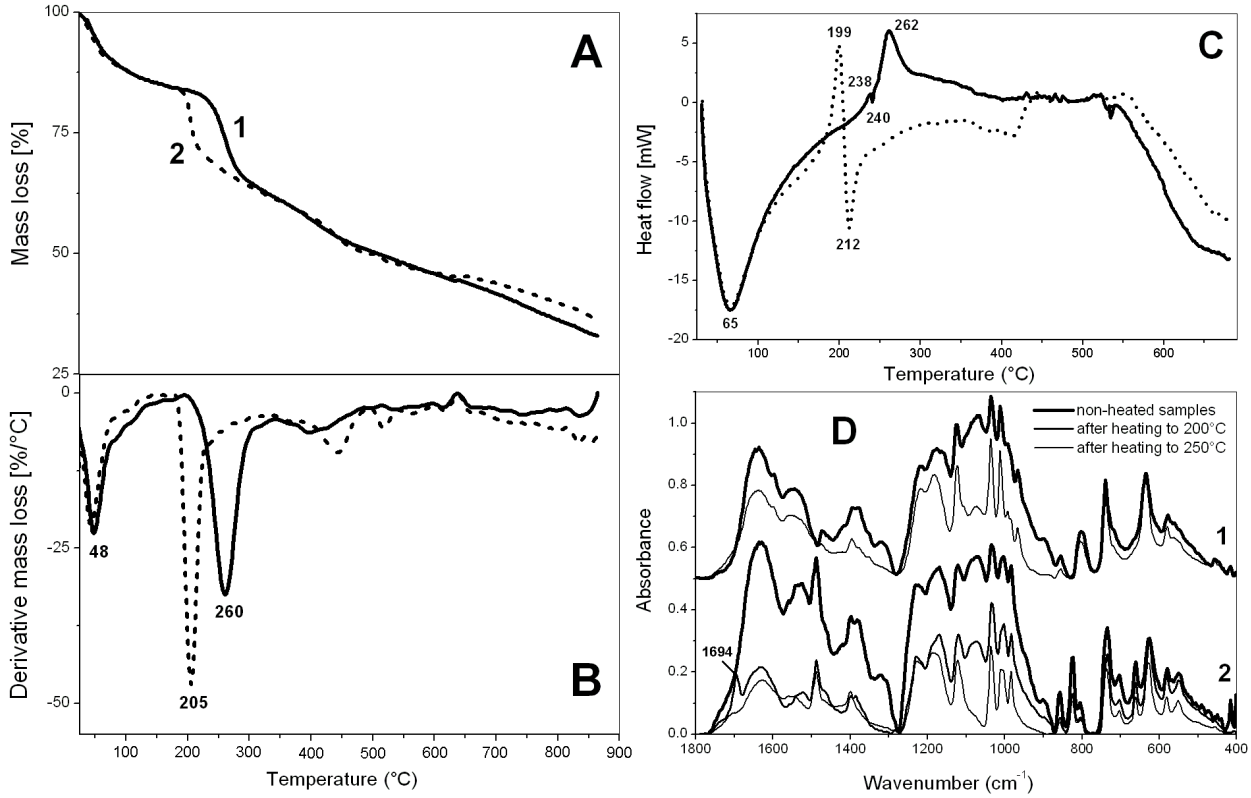

Figure 4 : TG (A), DTG (B) and DSC (C) curves of TPPS4/chitosan complexes **1** (solid) and **2** (dash); FT-IR spectra of the complexes after heating to 200 C (2) and 250 C (1 and 2) in comparing with corresponding non-heated samples

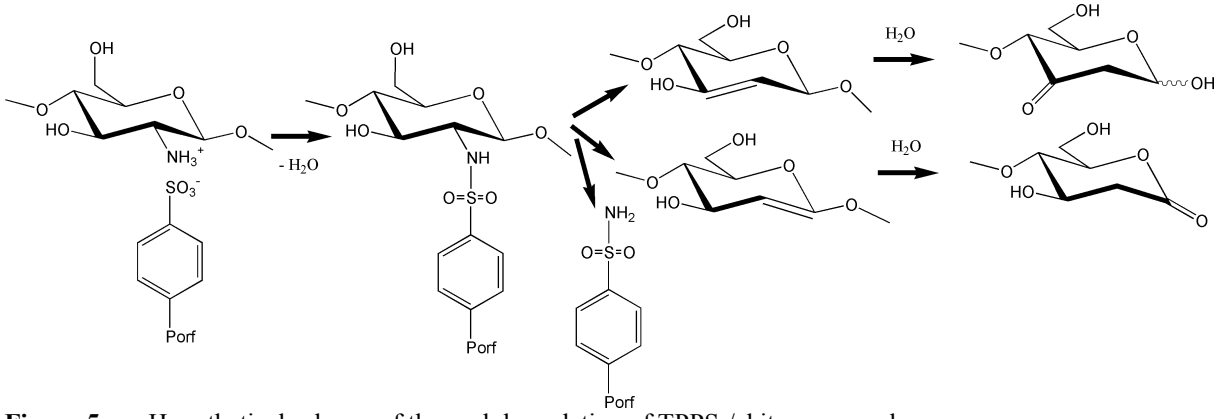

Figure 5 : Hypothetical scheme of thermal degradation of $TPPS_4$/chitosan complexes.

corresponding DSC peaks. As a result, the thermal stability decreases in the row chitosan–**1**–**2**. Decrease of thermostability observed for the complexes is a result of structural specificity of porphyrin-chitosan arrangement. In both cases, macrocyclic aggregates are inserted between chitosan macromolecules that weaken direct connection between polysaccharide chains. Thereby, the chitosan part of the complexes is more available to temperature treatment. The second thermal event for chitosan/$TPPS_4$ complexes occurs at lower temperatures (260 °C for **1** and 205 °C for **2**) than that of chitosan (310 °C). Corresponding DSC features are following: very weak exothermic/endothermic coupled peaks (238–240 °C) and broad exothermic peak (262 °C) for **1**, intense coupled exothermic (199 °C) and endothermic (212 °C) peaks for **2**. For the analysis of structural changes during thermal decomposition FT-IR spectra of the $TPPS_4$/chitosan complexes after heating to 200 a 250 °C were measured (Fig. 4 D). In both cases the significant decrease of the broad bands of the chitosan component was observed, while the intense and narrower bands of porphyrin showed no evident changes. An exception was two bands of **2** in the region of 420 – 400 cm^{-1}. Heating of complex **2** to 200 °C was accompanied by the rise of new band at 1694 cm^{-1}, which significantly declined after heating to 245 °C. This band assigned to C=O stretching

vibrations indicates the presence of carbonyl intermediates. We assume that the DSC couplet observed for the complexes may result from two-step pyrolysis of the ion complex structure porphyrin-SO_3^- $^+NH_3$-chitosan: (a) formation of sulphonamide linkages $–SO_2$-NH- (exothermic peak) and (b) pericyclic cis-elimination of porphyrin sulphonamide (endothermic peak). Carbonyl intermediates may appear by elimination of sulphonamide derivative of $TPPS_4$ and following hydrolysis of chitosan chain. The exo/endo couplet is much more pronounced for complex **2** confirming the prevalence of ionic cross-linking interactions between $TPPS_4$ and chitosan. Complex **1** showed only a slight couplet, so only small part of amino groups participate in electrostatic cross-linking to porphyrin. Similarly to chitosan, the exothermic peak of **1** may indicate thermal degradation of polysaccharide involving cross-linking reactions between the products of $–NH_2$ group pyrolysis.

Acknowledgements
This work was supported by the Ministry of Education of the Czech Republic (projects No. CEZ: MSM6046137305 and CEZ: MSM6046137307) and Grant Agency of the Czech Republic (525/05/0273).

References

[1] Al. Synytsya, An. Synytsya, P. Blafková, K. Volka, V. Král, Spectrochim Acta, in press (2006).

[2] J. Valančiunaite, J. Žerebcova, S. Bagdonas, G. Streckyte, R. Rotomskis, Lithuan. J. Phys, 44 (2004) 41-47.

[3] O. Ohno, Y. Kaizu, H. Kobayashi, J. Chem Phys, 99 (1993) 4128-4139.

[4] K. Kano, H. Minamizono, T. Kitae, S. Negi, J. Phys Chem, 101 (1997) 6118-6124.

[5] R. F. Khairutdinov, N. Serpone, J. Phys Chem, 103 (1999) 761-769.

[6] S. Gurrieri, A. Aliffi, E. Bellacchio, R. Lauceri, R. Purrello, Inorg Chim Acta, 286 (1999) 121-126.

[7] S. M. Andrade, S. M. Costa, J. Fluoresc, 12 (2002) 77-82.

[8] S. M. Andrade, S. M. Costa, Biophys J., 82 (2002) 1607-1619.

[9] X. Chen, M. Liu, J. Inorg Biochem, 94 (2003) 106-113.

[10] B. I. Iverson, K. Shreder, V. Král, P. Sansom, V. Lynch, J. Sessler, J. Am Chem Soc, 118 (1996) 1608-1616.

[11] B. I. Iverson, K. Shreder, V. Král, J. L. Sessler, J. Am Chem Soc, 115 (1993) 11022-11023.

[12] Al. Synytsya, V. Král, An. Synytsya, K. Volka, J. L. Sessler, Biochim Biophys Acta, 1620 (2003) 85-96.

[13] R. Bonnett, M. A. Krysteva, I. G. Lalov, S. V. Artarsky, Water Res, 40 (2006) 1269-1275.

[14] S. C. Tan, E. Khor, T. K. Tan, S. M. Wong, Talanta, 45 (1998) 713-719.

[15] Y.-H. Zhang, D.-M. Chen, T. He, F.-C. Liu, Spectrochim Acta Part A, 59 (2003) 87–101.

[16] X. Chen, M. Liu, J. Inorg Biochem, 94 (2003) 106-113.

[17] R. J. Abraham, G. E. Hawkes, M. F. Hudson, K. M. Smith, J. C. S. Perkin II (1974) 204-211.

[18] K. V. Harish Prashanth, F. S. Kittur and R. N. Tharanathan, Carbohydr Polym, 50 (2002) 27-33.